Applied Geochemistry 27 (2012) 1738–1744

Contents lists available at SciVerse ScienceDirect

Applied Geochemistry

journal homepage: www.elsevier.com/locate/apgeochem

Influence of pH and temperature on the early stage of mica alteration

K. Pachana [a,b], P. Zuddas [a,*,1], P. Censi [c]

[a] Institut de Génie de l'Environnement Ecodéveloppement & Département de Sciences de la Terre UMR 5125, Université Claude Bernard Lyon1, France
[b] Department of Chemistry, Burapha University, 169 Long-Hard Bangsaen Road, Chonburi 20131, Thailand
[c] Università di Palermo, Dipartimento DISTeM, via Archirafi 22, 90123 Palermo, Italy

ARTICLE INFO

Article history:
Available online 22 February 2012

ABSTRACT

Mineral dissolution and precipitation reactions actively participate in controlling fluid chemistry during water–rock interaction. In this study, the changes in the biotite and muscovite basal surface nano-morphology were evaluated during interaction with fluids of different pH (pH = 1.1, 3.3 and 5.7) at different temperatures (T = 25°, 120°, and 200 °C). Results show that at the nanometre scale resolution of the atomic force microscope (AFM), dissolution generates etch pits with a stair-shaped pattern over the (0 0 1) surface. The flux of dissolved elements decreases when pH increases. However, at pH 5.7, a change was found in the flux after 42 h of reaction when abundant gibbsite and kaolinite coat the dissolving mineral surface. This phenomenon was widely observed at edges of the etch pits by AFM. It was also found that an increase in temperature produces an enhancement in the elemental flux in both micas. Dissolution regime changes after less than one day of interaction at high temperature because of abundant coating formation over the etch pits and edges. The results demonstrate the key role of nanometre size neogenic phases in the control of elemental flux from mica surfaces to solution. The formation of nanometre size coatings, blocking the sites active for dissolution, appears to control the alteration of phyllosilicates even at the early stage of the interaction.

1. Introduction

To accurately estimate water quality evolution in many natural and human controlled processes it is prerequisite to understand the process of mineral alteration. Specifically, the ion release mechanism from silicates controls not only the pH of natural water but also the formation and stability of secondary minerals as well as the mobility of potential harmful and toxic metals. The hydrothermal alteration of minerals is important to a wide range of basic and industrial processes. In recent years, the quantitative evaluation of the hydrothermal alteration of minerals has become crucial in establishing the economic and security feasibility of CO_2 storage in geological reservoirs (Kharaka et al., 2009). More recently, the re-evaluation of global geothermal resources also requires a greater understanding of mineral alteration and stability (Morgillo and Axelsson, 2010, and references therein).

In the particular case of phyllosilicates, the alteration of mica is considered to be the general pathway in the formation of vermiculite and smectite. These clay minerals generate the material responsible for changing rock structure and sediment porosity via the formation of several kinds of cement. In geothermal systems, mica dissolution results in forming illite and smectite that in turn promote pressure solution in sedimentary basins (Gerard et al., 2002; Meyer et al., 2006). Although the understanding of mica alteration is crucial to the dynamics of water–rock interaction, studies on mica dissolution mechanisms are rare (Nickel, 1973; Lin and Clemency, 1981; Knauss and Wolery, 1989; Tulpault and Trotignon, 1994; Oelkers et al., 2008). These studies suggest that mica dissolution rates vary as a function of pH much as they do in other aluminosilicates: dissolution rates decrease with increasing pH under acid conditions, and are minimal at near neutral pH, while they increase as pH reaches basic values. Among other aspects of mica dissolution, Dietzel (2000) and Maurice et al. (2002) investigated the degree of Si polymerisation during muscovite dissolution at a pH of 3. Studies on mica surface reactivity have been reviewed by Nagy (1995).

This study builds upon this past work by focusing on the effect of reactive solution composition and temperature at the mica–water interface. Reactions at this interface play a role in a number of natural processes. The focus was on the reaction mechanisms occurring at the surface of the mineral during the first stage of the reaction. Micas are layer phyllosilicates consisting of two tetrahedral (T) sheets with an octahedral (O) sheet in between (TOT structure). The octahedral unit is linked to the others by sharing octahedral edges. In biotite all the three octahedral sites are occupied by chemical elements (trioctahedral) whereas, in muscovite only two octahedral sites are occupied (dioctahedral). Since the 2:1 structure is negatively charged, an interlayer cation neutralises

* Corresponding author.
E-mail address: pierpaolo.zuddas@upmc.fr (P. Zuddas).
[1] Present address: Université Pierre te Marie Curie, Paris-Sorbonne, ISTEP, 4 place Jussieu, F75005 Paris, France.

0883-2927/$ - see front matter © 2012 Elsevier Ltd. All rights reserved.
doi:10.1016/j.apgeochem.2012.02.009

the bulk electrical structure. Biotite is a mica that has K^+ as an interlayer cation, Mg and Fe are in the trioctahedral layer and Si and Al make up the tetrahedral layer. Muscovite has a similar structure except that it contains Al in the dioctahedral layer. There are two main types of mica surface: the basal (0 0 l) parallel to the layers and the lateral (hk0) (Nagy, 1995). Basal (0 0 1) surfaces are composed of many tetrahedral units joined by shared O atoms at their corners. If a mica monocrystal is cleaved, the (0 0 l) basal face may contain K ions on the tetrahedral sheet. In contrast, lateral (hk0) surfaces consist of TOT and of K^+ interlayers between two TOT units with a potential different reactivity.

2. Experimental conditions

2.1. Materials

The mechanism of biotite and muscovite alteration at the (0 0 l) basal face was investigated combining atomic force microscopy (AFM) observations and analysis of the chemical composition of the interacting solutions. A large monocrystal of muscovite from South India and a biotite crystal from Sweden (mineralogical collection of the University of Lyon) were selected for this study. The bulk analysis of the samples by X-ray fluorescence spectroscopy gave the following chemical formula estimates: $K(Mg_{2.5}\ Fe^{2+}_{0.05}Fe^{3+}_{0.2})(Si_{2.9}Al_{1.1})O_{10}(OH)_4$ (biotite) and $K(Fe_{0.02}Al_{1.98})(Si_{3.18}Al_{0.82})O_{10}(OH)_4$ (muscovite).

Solutions of a given pH were prepared by adding suprapure HCl to Milli-Q deionised water at room temperature. Different pH and temperature conditions were investigated.

2.2. Methods

The influence of pH and temperature on the mica alteration process were investigated using a 1 × 1 × 0.1 cm monocrystal of mica placed in contact with 10 mL of solution in a PTFE tube cell at varying initial pH values: 1.1, 3.3 and 5.7. The investigated reaction time varied between 30 min and 7 days. After reaction, the solution from each cell was collected using a syringe and filtered through a 0.2 μm pore-size Minisarter filter. Sampled solutions were divided into two aliquots: one for silicon analysis and pH control and the second for the analysis of the other elements. The morphological surface state (0 0 1) was determined by scanning electron microscopy (SEM) and atomic force microscopy (AFM).

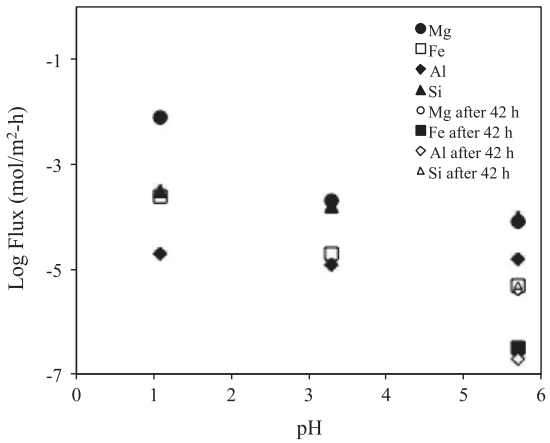

Fig. 2. Fluxes of Mg, Al, Fe and Si (on logarithmic scale) as a function of pH at the temperature of 25 °C during the experiment on biotite alteration. A change is observed after 42 h of interaction at pH 5.7.

The influence of temperature was investigated by experiments where mica monocrystals and aqueous solutions at pH 3.3 were introduced into PTFE cells placed in steel autoclaves stored in an oven at constant temperature. A pH of 3.3 was chosen because at that pH dissolved Al generally begins to precipitate. A more detailed description of the experimental apparatus has been presented previously (Zuddas and Michard, 1993). Experiments were conducted at three different temperatures, 25° ± 2, 120° ± 3, 200° ± 4 Celsius, and for an identical vapour saturation pressure. The cell (containing the mineral and solution) was weighed before and after reaction to evaluate the possible loss of solution by evaporation. After reaction, each cell was cooled to ambient temperature. Solutions were sampled using a protocol identical to the pH investigation. The mineral surface was observed by SEM and AFM.

2.3. Analysis

Solution pH was measured at 25 °C with an Ingold electrode calibrated against NIST traceable buffer solutions (pH 4.01 and 7.01 at

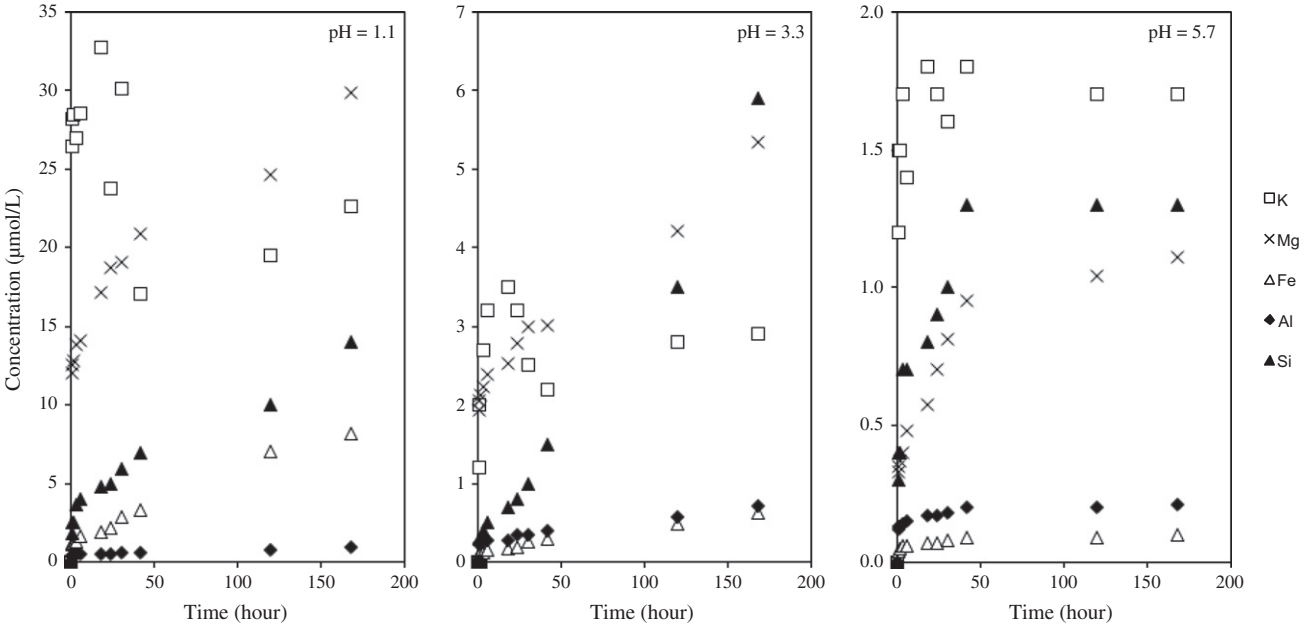

Fig. 1. Concentration of dissolved elements as a function of time at different pH conditions during the experimental biotite alteration.

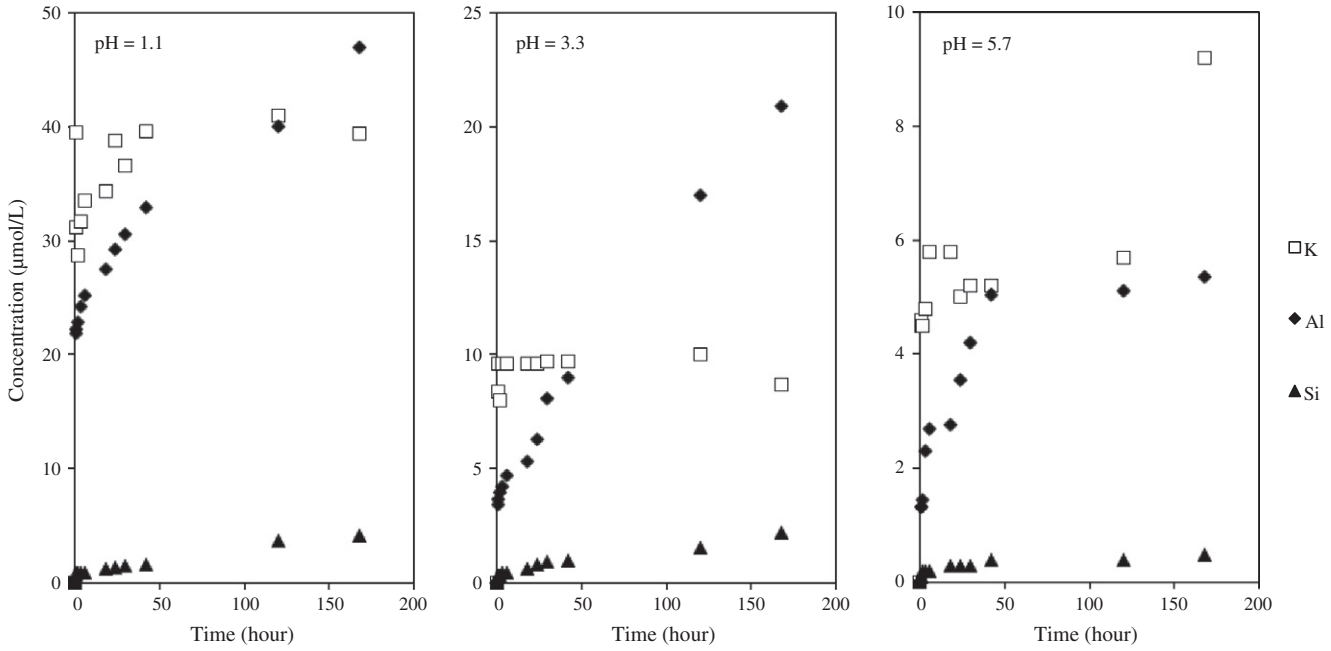

Fig. 3. Concentration of dissolved elements as a function of time at different pH conditions during the experiment on muscovite alteration.

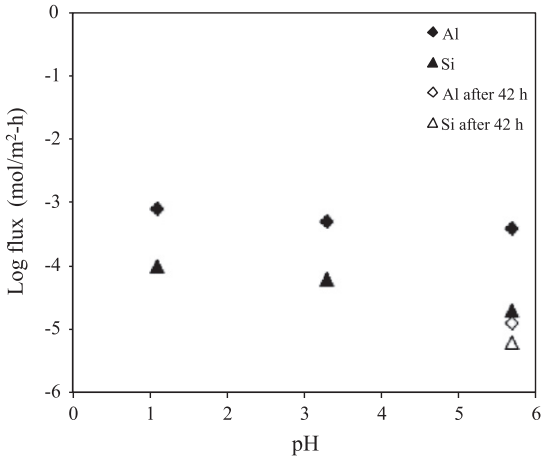

Fig. 4. Fluxes of Al and Si (on logarithmic scale) as a function of pH at the temperature of 25 °C during the experiment on muscovite alteration. A change is observed after 42 h of interaction at pH 5.7.

25 °C). An automatic colorimeter was used to measure dissolved Si. Aluminium and Fe were determined by Graphite Furnace Atomic Adsorption Spectroscopy, and Mg and K by Inductively Coupled Plasma-Mass Spectrometry and Flame Atomic Absorption Spectroscopy, respectively. The analytical precision value was 2–3% for Si, 5% for K and Mg, and 10% for Al and Fe.

The mica surface was analysed by AFM. The images were collected after 168 h of reaction using a molecular imaging AFM (Nanoscope III) equipped with Digital Instrument software and a 7.5 µm × 7.5 µm scanner. AFM operated in contact mode and at an imaging loading force ⩽10 nN using a silicon probe with a spring constant of 0.02–0.1 N/m. The scan frequency was 4 Hz with 256 lines per scan while the elapsed time from the top to the bottom of each image was about 1 min. To exclude the possibility of dirty tip formation, the scan angle was rotated during image collection and a highly ordered pyrolitic graphite (HOPG) standard was used as a control.

2.4. Estimation of the cation flux

The flux of cation in solution was estimated by:

$$\Phi_{(x)} = \frac{\Delta C_x(\text{mol})}{\Delta t(h) \times \text{surface}(m^2)} \quad (1)$$

where $\Delta C/\Delta t$ (mol/h) is the variation of the concentration C of elements (Si, Al, K) over the range of time t and surface is the geometric surface area estimated by the summation of width and length multiplication of each crystal's initial surface. Since the K flux may depend on exchange reactions with solution H^+, the K flux was not estimated (Acker and Bricker, 1992).

3. Results

3.1. The influence of pH on flux

Results reported in Annexe 1 show that pH values measured at the beginning and the end of the reaction time are the same. This indicates that the hydrothermal experimental reaction investigated in this study takes place under constant pH conditions.

3.1.1. Biotite

Fig. 1 shows the evolution of the dissolved elements as a function of time during biotite dissolution at different pH conditions. Potassium was present at a higher concentration compared to the other dissolved elements in the first 42 h of investigation. In experiments at pH 1.1 and 3.3, the concentration of Si, Al, Fe and Mg constantly increased as a function time, while in experiments at pH 5.7, solutions reached a steady state after 42 h of reaction for Al, Si and Mg. The saturation state of the solution was estimated using the PHREEQC software (Parkhurst and Appelo, 1999) and it was found that at pH 5.7, fluids were oversaturated with respect to gibbsite ($Al(OH)_3$) after only 42 h of reaction.

In plotting the flux of elements on a logarithmic scale as a function of pH for the first 42 h of reaction (Fig. 2), was found that Si and Al fluxes decreased 3–4-fold when pH increased from 1.1 to 5.7, while Fe and Mg fluxes decreased 2- and 1-fold, respectively.

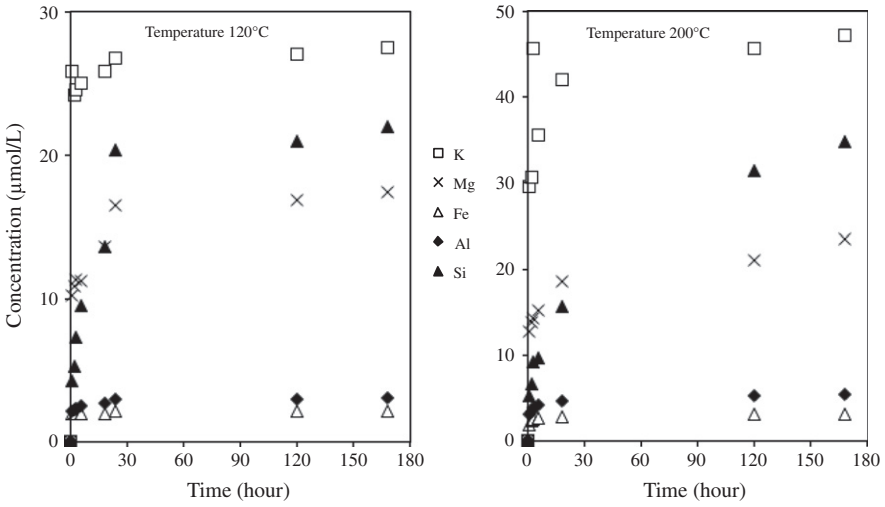

Fig. 5. Concentration of dissolved elements as a function of time during the experiment on biotite alteration at pH 3.3 and at different temperatures.

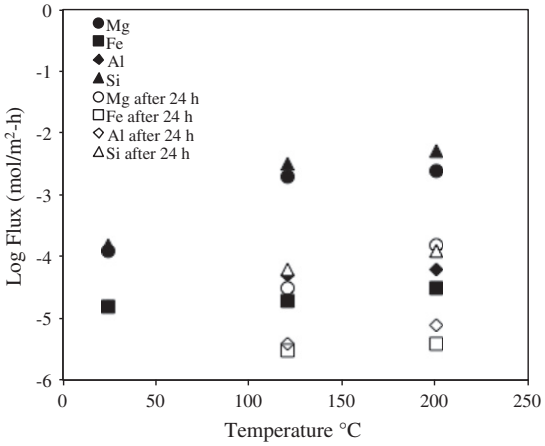

Fig. 6. Fluxes of Mg, Al, Fe and Si (on logarithmic scale) as a function of temperature during the experiment on biotite alteration at pH 3.3. At both 120 and 200 °C, fluxes change after 24 h of interaction.

In experiments at pH 5.7 two flux regimes were identified: one before and one after 42 h of reaction. After 42 h of reaction, Si and Al fluxes decreased by 2 orders of magnitude while Mg and Fe fluxes decreased by 3 orders of magnitude.

3.1.2. Muscovite

Fig. 3 shows the evolution of K, Al, and Si concentrations as a function of time at the different pH values. Potassium remained nearly constant throughout the 168 h of investigation at all the investigated pH values. At pH 1.1 and 3.3, Si and Al concentrations increased linearly as a function of time. At pH 5.7, Al decreased after 42 h of reaction. The decrease in Al concentration could be related to the precipitation of secondary minerals. Modelling the solution saturation state, it was found that after 42 h of reaction, fluids were saturated with respect to gibbsite, kaolinite [$A_2Si_2(OH)_4$] and boehmite [AlO(OH)].

Fig. 4 shows that in the first stage of the reaction, the Al flux remained constant when pH increased while Si decreased by an order of magnitude. At pH 5.7 and after 42 h of reaction, Si and Al fluxes were 2 orders of magnitude lower compared to the earlier stage.

3.2. Influence of temperature on flux

3.2.1. Biotite

Fig. 5 shows that Al, Si, Fe and Mg concentrations increased as a function of time during the first 24 h of investigation, and afterwards reached a steady state. In batch experiments, steady state may reflect either isochemical mineral dissolution–precipitation reactions (Pauwels et al., 1989) or a lower dissolution rate of parent minerals. Under the experimental conditions, it was found that at steady state, the solutions are oversaturated with respect to both kaolinite and gibbsite. This suggests the possible precipitation of neogenic phases potentially able to cover part of the dissolving mica surface.

Fig. 6 shows that in the first 24 h, the flux of Fe increased slightly, while Al, Mg and Si increased by 1–2 orders of magnitude when temperature increased from 25 to 200 °C. After 24 h of reaction however, fluxes of Al, Fe and Mg decreased by more than 1 order of magnitude as temperature increased from 25 to 200 °C. Silicon flux decreased when temperatures increased from 25 to 120 °C and increased by an order of magnitude when temperature increased from 120 to 200 °C.

3.2.2. Muscovite

Fig. 7 shows K, Al, and Si concentrations as a function of time at 120 and 200 °C. It was found that K concentration was higher than Al and Si. At both 120 and 200 °C, Al and Si concentrations increased constantly as a function of time in the first 18 h and later reached steady state. A similar trend was observed during the hydrothermal alteration of biotite. In muscovite however, steady state is reached earlier than in the biotite experiments. After 18 h of reaction, fluids were saturated with respect to both gibbsite and kaolinite.

It was found that Al and Si fluxes were constant at 25 °C during the 168 h of investigation, similar to the findings for biotite alteration. However, at both 120 and 200 °C two distinct trends were identified, one before and the other after 18 h of reaction. In the first stage, Al and Si fluxes increased by 2 orders of magnitude as a function of temperature increase while in the second stage, Al and Si fluxes decreased by 2 orders of magnitude at 120 and 200 °C (Fig. 8).

3.3. Evolution of the surface state

The state of the pristine surface after air cleavage and before the experiment was found to be perfectly flat with surface roughness

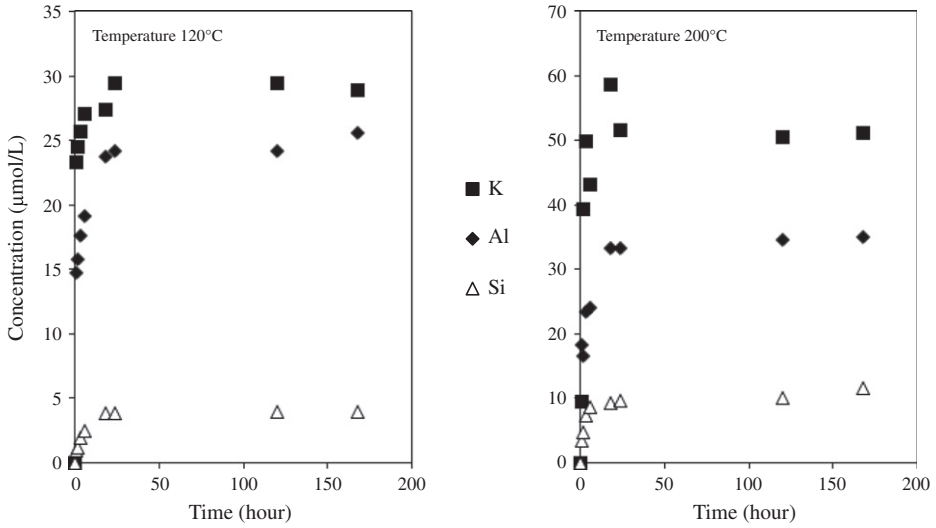

Fig. 7. Concentration of dissolved elements as a function of time during the experiment on muscovite alteration at pH 3.3 and at different temperatures.

values lower than 0.1 ± 0.1 nm as measured by AFM. No evidence of defect points or dislocations was observed. The determinations confirm earlier AFM investigations on layer silicate minerals (Henderson et al., 1994) where it was found that freshly cleaved mica surfaces are perfectly flat at the atomic scale resolution of the basal (0 0 1) surface (Coleman et al., 1993; Baba et al., 1997; Campbell et al., 1998).

After 168 h of reaction, SEM observations show the presence of etch pits on the biotite basal surface interacting with solutions at pH = 3.3 and 200 °C. Pits have circular form and appear randomly distributed over the surface. This confirms previous work on silicate alteration (Zuddas and Michard, 1993; Murakami et al., 2002; Aldushin et al., 2006), where dissolution effects on the surface state were found from the very early stages of the process. However, the relationship between the measured dissolution fluxes and surface changes is unclear.

To better characterise the relationship between flux and surface behaviour during hydrothermal alteration of mica, AFM high-resolution equipment was used rather than the SEM. It was found that on the basal (0 0 1) surface of both biotite and muscovite, etch pits have a stair shaped pattern as shown in Fig. 9. Measuring the thickness of the first step in several etch pits, values of 4.4 ± 0.5 and 4.5 ± 0.5 Å were found for biotite and muscovite, respectively. These values are in agreement with the theoretical thickness of tetrahedral and octahedral sheet summation of both micas, showing the potential structural control of the dissolution during the early stage of muscovite and biotite dissolution under acidic conditions.

Fig. 10 shows the presence of nano-coatings at the surface edge of triangular pits during the biotite and muscovite experiments after 168 h of reaction. Here, neogenic phases may coat the surface of the dissolving mica, explaining the significant decreases in elemental flux observed in the reacting fluids. It was found that the etch pit density was higher at pH 1.1 compared to pH 3.3 or 5.7, while the amount of neogenic coatings present at the surface edge of the steps was significantly higher at pH 5.7 compared to that observed at pH 1.1 and 3.3.

4. Discussion

This experimental study confirms that pH controls the flux of dissolved elements during hydrothermal alteration of mica under acidic and far from equilibrium conditions. The release of elements from mica to the solution decreases by 2 orders of magnitude when pH increases from 1 to 5.7. Nanometre scale observations carried out on mica surfaces indicate that the density of etch pits decreases when pH increases from 1.1 to 5.7. This shows that as pH increases, the available reactive surface decreases confirming previous studies where it was postulated that mica dissolution depends on H^+ activity (Bales and Morgan, 1985; Carrol-Webb and Walther, 1988; Acker and Bricker, 1992; Casey et al., 1993; Kalinowski and Schweda, 1996; Oelkers et al., 2008).

According to the Transition State Theory, when a mica crystal is in contact with solutions, H^+ may exchange with K^+ to form an activated complex with surface cations leading to polarisation and instability of cationic bonds with the mineral surface (Stumm and Wollast, 1990). Theoretically, this instability should facilitate the detachment of cations from the mica surface and their transfer into solution. Under acidic and far from equilibrium conditions, as H^+ activity increases so does surface instability. This 'activated complex' itself is not stable and is released rapidly. Moreover, the AFM observations of the basal (0 0 1) mica surfaces showed that etch pits have a stair pattern suggesting the higher reactivity of the lateral surfaces. In both biotite and muscovite, lateral (1 1 0) faces are characterised by under-saturated O bonds leading to faster dissolution compared to the basal faces where O bonds are saturated. The full charge of O atoms at the basal surface has a lower affinity for protonation.

The result of this study shows that dissolution of mica is not congruent: Mg/Si, Fe/Si and Al/Si ratios in solutions are higher compared to ratios in both biotite and muscovite minerals. The elemental flux is not only dependent on pH but also results from the precipitation of neogenic minerals coating pit edges and lateral surfaces. The observed change in flux after 42 h of reaction at pH 5.7 reflects the precipitation of neogenic phases as confirmed by high-resolution AFM surface observations. SEM does not reveal the coating phenomenon; the same surfaces observed with SEM appear to be flat. The nanometre scale observations clearly indicated that coatings block the reactive sites of the mica surfaces controlling the reaction time of mica dissolution. It is proposed that coating formation inhibits H^+ interaction with under-saturated O atoms at the highly reactive pit edges and lateral surfaces. Elemental flux is then slowed because the available reactive surface is reduced.

This study shows that the flux of dissolved elements increases when the temperature increases confirming the catalytic role played by temperature. At higher temperatures mica is more

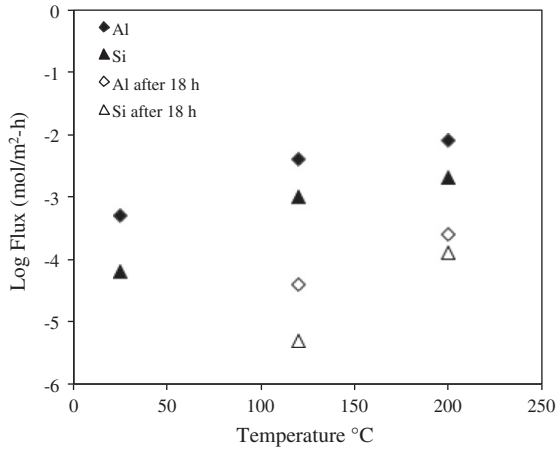

Fig. 8. Fluxes of Al and Si (on logarithmic scale) as a function of temperature during the experiment on muscovite alteration at pH 3.3. At both 120 and 200 °C, fluxes change after 18 h of interaction.

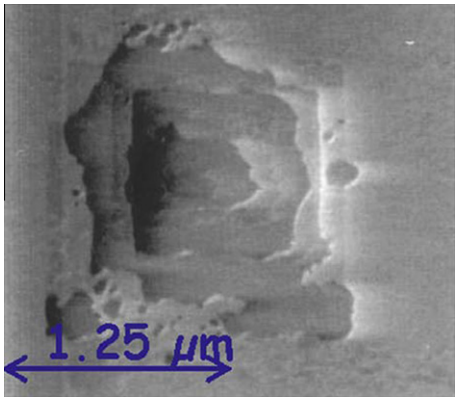

Fig. 9. Atomic force microscopy detailed images of the etch pit shape observed on the basal (0 0 1) surface of biotite during the hydrothermal alteration at pH 3.3 and 200 °C after 168 h of reaction.

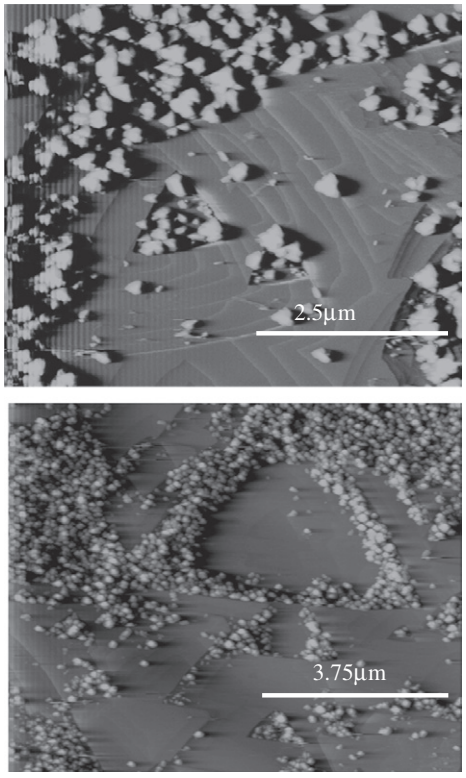

Fig. 10. Atomic Force Microscopy overall images of the basal (0 0 l) mica surfaces after 168 h of interaction with fluids at pH 3.3 at the temperature of 200 °C. (Top: muscovite; bottom: biotite.)

energetic and surface cations are activated generating more collisions with solutions. This greater instability of cationic bonds at the mineral surface facilitates ion detachment (Stumm and Morgan, 1980). It was found that the precipitation of neogenic phases reduces the elemental flux. The surface observations at the end of the experiment showed neogenic phases coating both muscovite and biotite. They were particularly abundant at the edge and lateral surfaces at 120 and 200 °C. It is propose that in long term interaction, higher temperature may initially accelerate dissolution and facilitate the formation of neogenic phases. Over time, the neogenic phase coatings inhibit mica alteration.

The study demonstrates the pre-eminent role of neogenic mineral coatings in the control of elemental flux. Mineral dissolution accelerators such as low pH and high temperatures may also enhance coating formation. The phenomena documented in the experimental conditions have also been described in natural buried feldspars (Nugent et al., 1998; Murakami et al., 1998, 2002). Under natural conditions, coating formation can also be facilitated by closed system conditions and a low water–rock ratio.

5. Implications and conclusions

There are major discrepancies between the mineral dissolution rates documented in laboratory experiments and those observed in the natural watershed. This is because it is not possible to determine precisely the reactive surface area between minerals and the percolating waters in rocks and soils under natural conditions. Mineral alteration is not a homogeneous process because coatings may cover the mineral surface from the earliest stages of water–mineral interaction. By proving the early formation of surface coatings, this study indicates that when applying experimental determination to natural situations account must be taken of the real state of the mineral surface. Naturally occurring mineral surfaces are not pure phases; they may be mixtures of various minerals and they have most often been altered by the formation of coatings.

The results have implications on the definition of the reactive surface area of minerals. The available reactive surface area is not the total geometric surface of the minerals but rather the sum of the sites that actually reacted with the nearby aqueous solution (see Brantley et al. (2008) for a review). An explanation is provided for the variation of dissolution fluxes during mica alteration through analysis of the nanometre details of the reacting mineral surfaces. The loss of matter from the mineral surface is governed by the formation of stair-shaped etch pits. The density of steps and etch pits over the surface increases as pH and temperature increase. However, the study has provided direct observations demonstrating that active surface sites of both dioctahedral and trioctahedral mica have a temporal dependence due to the rapid formation of nanometre coatings that block the dissolution reactive sites.

Finally, results of this experimental study may improve the quantitative assessing of the ability of minerals to neutralise CO_2 acidic fluids. At the initial stage of the interaction, when minerals dissolve abundantly, CO_2 can be easily captured in the form of HCO_3^- ions, but when coatings form at the mineral surface, the mineral's capacity to neutralise the acidity of the fluid decreases significantly or can be brought to a halt. Predictive modelling of

CO_2 sequestration under geological conditions should take into account the inhibiting role of surface coating formation. This work may open the door to a new generation of rate equations and modelling concepts for a better understanding and prevision of how minerals dissolve and influence the environment.

Acknowledgments

We thank Ekhard Salje, Pierre Toulhoat, Giovanni De Giudici, Olivier Lopez and Pichan Sawangwong for helpful discussions during the course of this study. Eva Deliry and Dominique Lavergne provided technical assistance. We also thank Prof. R. Cidu and two anonymous reviewers for their important contribution that significantly improved the quality of the manuscript and Robin Silver for her assistance in English-language editing. Financial support was provided principally by the University of Lyon.

Appendix A. Supplementary material

Supplementary data associated with this article can be found, in the online version, at doi:10.1016/j.apgeochem.2012.02.009.

References

Acker, J.G., Bricker, O.P., 1992. The influence of pH on biotite dissolution and alteration kinetics at low temperature. Geochim. Cosmochim. Acta 56, 3073–3092.

Aldushin, K., Jordan, G., Schmahl, W., 2006. Basal plane reactivity of phyllosilicate studied in situ by hydrothermal atomic force microscopy (HAFM). Geochim. Cosmochim. Acta 70, 4380–4391.

Baba, M., Kakitani, S., Ishii, H., Okuno, T., 1997. Fine atomic images of mica cleavage planes obtained with an atomic force microscope (AFM) and a novel procedure for image processing. Chem. Phys. 221, 23–31.

Bales, R.C., Morgan, J.J., 1985. Dissolution kinetics of chrysotile at pH 7–10. Geochim. Cosmochim. Acta 49, 2281–2288.

Brantley, S.L., Kubicki, J.D., White, A.F., 2008. Kinetics of Water–Rock Interaction. Springer.

Campbell, P.A., Sinnamon, L.J., Thompson, C.E., Walmsley, D.G., 1998. Atomic force microscopy evidence for K^+ domains on freshly cleaved mica. Surface Sci. 410, 768–772.

Carrol-Webb, S.A., Walther, J.V., 1988. A surface complexation reaction model for pH dependence of corundum and kaolinite dissolution rates. Geochim. Cosmochim. Acta 52, 2609–2623.

Casey, W.H., Banfield, F.J., Westrich, R.H., Linda, M., 1993. What do dissolution experiments tell us about natural weathering? Chem. Geol. 105, 1–15.

Coleman, R.V., Xue, Q., Gong, Y., Price, P.B., 1993. Atomic force microscope study of etched tracks of low-energy heavy ions in mica. Surface Sci. 297, 359–370.

Dietzel, M., 2000. Dissolution of silicates and the stability of polysilicic acid. Geochim. Cosmochim. Acta 64, 3275–3281.

Gerard, F., François, M., Ranger, J., 2002. Processes controlling silica concentration in leaching and capillary soil solutions of and acidic brown forest soil (Rhône, France). Geoderma 107, 197–226.

Henderson, G.S., Vrdoljak, R.K., Wicks, F.J., Rachlin, A.L., 1994. Atomic force microscopy studies of layer minerals. Coll. Surf. A: Physicochem. Eng. Aspects 87, 197–212.

Kalinowski, B.E., Schweda, P., 1996. Kinetics of muscovite, phlogopite, and biotite dissolution alteration at pH 1–4, room temperature. Geochim. Cosmochim. Acta 60, 367–385.

Kharaka, Y.K., Thordsen, J.J., Hovorka, S.D., Nance, H.S., Cole, D.R., Phelps, T.J., Knauss, K.G., 2009. Potential environmental issues of CO_2-storage in deep saline aquifers: geochemical results from Frio-I pilot test, Texas, USA. Appl. Geochem. 26, 1106–1112.

Knauss, K.G., Wolery, T.J., 1989. Muscovite dissolution kinetics as function of pH and time at 70 °C. Geochim. Cosmochim Acta 53, 1493–1502.

Lin, F.C., Clemency, C.V., 1981. The kinetics of dissolution of muscovite at 25 °C and 1 atm CO_2 partial pressure. Geochim. Cosmochim. Acta 50, 1667–1677.

Maurice, P.A., McKnight, D.M., Leff, L., Fulghum, J.E., Gooseff, M., 2002. Direct observations of aluminosilicate weathering in the hyporheic zone of an Antartic Dry Vallen Stream. Geochim. Cosmochim. Acta 66, 1335–1347.

Meyer, E.E., Greene, G.W., Alcantar, N.A., Isrealachvili, J.N., Boles, J.R., 2006. Experimental investigation of the dissolution of quartz by a muscovite mica surface. Implication for the pressure solution. J. Geophys. Res. Solid Earth 111, B08202.

Morgillo, M.A., Axelsson, G., 2010. Preface to geothermal special issue on sustainable geothermal utilisation. Geothermics 39, 279–282.

Murakami, T., Kogure, T., Kadohara, H., Ohnuki, T., 1998. Formation of secondary mineral and its effect on anorthite dissolution. Am. Mineral. 83, 1209–1219.

Murakami, T., Utsonomiya, S., Yokoyama, T., Kasama, T., 2002. Biotite dissolution processes and mechanisms in the laboratory and nature: early stage weathering environment and vermiculization. Am. Mineral. 83, 1209–1219.

Nagy, K.L., 1995. Dissolution and precipitation kinetics of sheet silicates. Rev. Mineral. 31, 173–233.

Nickel, E., 1973. Experimental dissolution of light and heavy minerals in comparison with weathering and intrastratal solution. Contribut. Sediment. 1, 1–68.

Nugent, M.A., Brantley, S.L., Pantano, C.G., Maurice, P.A., 1998. The influence of natural mineral coatings on feldspar weathering. Nature 395, 588–591.

Oelkers, E., Schott, J., Guathier, J.M., Herrero-Roncal, T., 2008. An experimental study of the dissolution mechanism and rates of muscovite. Geochem. Cosmochim. Acta 72, 4948–4961.

Parkhurst, D.L., Appelo, C.A.J., 1999. User's guide to PHREEQC (version 2)-A computer program for speciation, batch-reaction, one-dimensional transport, and inverse geochemical calculations. US Geol. Surv. Water-Resour. Invest. Rep. 99-4259.

Pauwels, H., Zuddas, P., Michard, G., 1989. Behaviour of trace elements during feldspar dissolution in near equilibrium conditions: preliminary results. Chem. Geol. 78, 257–267.

Stumm, W., Morgan, J.J., 1980. A ligand exchange model for the adsorption of inorganic and organic ligand at hydrous oxide interface. Croat. Chim. Acta 53, 291–312.

Stumm, W., Wollast, R., 1990. Coordination chemistry weathering: kinetics of surface controlled dissolution of oxide minerals. Rev. Geophys. 23, 53–69.

Tulpault, M.P., Trotignon, L., 1994. The dissolution of biotite single crystals in dilute HNO_3 at 24 °C: evidence of anisotropic corrosion process of micas in acidic solutions. Geochim. Cosmochim. Acta 56, 3312-3122.

Zuddas, P., Michard, G., 1993. Experimental mineral–fluid interaction in the Ca–Na–(Sr)–Al–Si system. Eur. J. Mineral. 5, 807–818.